http://doi.org/10.35784/iapgos.6051 *received: 29.03.2024 | revised: 21.11.2024 | accepted: 23.11.2024 | available online: 21.12.2024*

# STUDY OF THE OZONE CONTROL PROCESS USING ELECTRONIC SENSORS

**Sunggat Marxuly[1], Askar Abdykadyrov[1], Katipa Chezhimbayeva[2], Nurzhigit Smailov[1]**
[1]Kazakh National Research Technical University named K. Satbayev, Department of Electronics, Telecommunications and Space Technologies, Almaty, Kazakhstan, [2]Almaty University of Power Engineering and Telecommunications named after G.Daukeev, Department of Electric Drive and Automation of Industrial installations, Almaty, Kazakhstan

***Abstract.*** *In research work the problem of studying the process of ozone control with the help of electronic sensors is considered. In research work, special sensors were used, which are formed around coronary electrodes in the ozonator and to monitor the concentration of ozone in the room. This is because ozone is known to adversely affect human health if its maximum permissible air concentration exceeds 0.16 mg/m$^3$. A small system of ozonators was developed in a special laboratory, theoretical and experimental tests were carried out. In practice, the obtained data and the electric diagram of the ozonator (on the ARDUINO platform) were collected. "Prana Air" sensors and current sensors were used to accurately determine the ozone ($O_3$) concentration around the ozone nozzle to measure the current at the electrodes.*

**Keywords**: ozone control, sensors, control systems, electric discharge, machine learning, monitoring

## BADANIE PROCESU KONTROLI OZONU ZA POMOCĄ CZUJNIKÓW ELEKTRONICZNYCH

***Streszczenie.*** *W pracy rozważono problem badania procesu kontroli ozonu za pomocą elektronicznych czujników. W badaniach zastosowano specjalne czujniki, które są rozmieszczone wokół elektrod koronowych w ozonatorze, aby monitorować stężenie ozonu w pomieszczeniu. Jest to istotne, ponieważ wiadomo, że ozon negatywnie wpływa na zdrowie człowieka, jeśli jego maksymalne stężenie w powietrzu przekracza 0,16 mg/m³. W specjalistycznym laboratorium opracowano niewielki system ozonatorów oraz przeprowadzono testy teoretyczne i eksperymentalne. W praktyce zebrano uzyskane dane oraz schemat elektryczny ozonatora (na platformie ARDUINO). Do dokładnego określenia stężenia ozonu ($O_3$) wokół dyszy ozonowej oraz do pomiaru prądu na elektrodach zastosowano czujniki "Prana Air" oraz czujniki prądu.*

**Słowa kluczowe**: kontrola ozonu, czujniki, systemy sterowania, wyładowania elektryczne, uczenie maszynowe, monitoring

## Introduction

To study the process of controlling the operation of the ozonator using electronic sensors, it is advisable to first consider the specific chemical and physical properties of ozone. Ozone is an allotropic species change in oxygen, the chemical formula of which is $O_3$. The color is dark blue, a pungent-smelling gas, and liquid ozone is purple blue; the melting point is t – 192.7°C, the boiling point is T – 112°C. the solubility in water is 0.394 g/l (at 0°C). Ozone is unstable, spontaneously releases heat and turns into oxygen [20]. The maximum allowable concentration of ozone in the air is 0.16 mg/m$^3$. If the concentration of ozone in the air is higher than the amount of MPC, then a person's airway narrows and suffers from headaches [23]. The concentration of ozone in the air is very unstable due to temperature, its life time is tens of seconds. That is, it is known that ozone is converted back into oxygen ($O_2$) [10].

Today, even in industrialized countries, ozone pollution in the tropospheric air is one of the main problems that is increasing every day [37]. Environmental pollutants and various gases consist of three main sources: transport, heat, industry. In addition to these common sources, climate changes and air pollution also have interrelated effects [36]. High concentrations of air pollution continue to have a significant impact on human health. Ozone pollution negative impact on human health and ecosystem is one of the most important pollutants [26].

Alexandru C. Fechete and his colleagues developed ozone sensors using devices based on the surface acoustic wave (SAW). The structure of the sensors in it consists of a lithium tantalate piezoelectric ($LiTaO_3$) substrate with an intermediate layer of silicon nitride ($SiN_x$). The research paper proposes a comparative discussion of the performance of sensors in terms of response time, recovery time and response magnitude as a function of operating temperature. A particularly large frequency shift of up to 56 kHz was observed for the concentration of $O_3$ in the air. The microstructural characteristics of InOx thin films are also determined by atomic strength microscopy (AFM) [12, 24].

In a domestic home environment with ozone [17] the success of the process of decontaminating any product or air in the same way as water depends on some variables: gas concentration, temperature, pressure and humidity. When these variables are monitored and stored remotely, data redundancy and operational security increase. For this purpose, the benefits of using airborne ozone wireless sensor [19] networks are a technological alternative. Gerson Roberto Luqueta and his colleagues considered the input and analysis of data from wireless sensor network configurations in the control of the process of ozone neutralization [22]. There you can track important variables and keep records of them. In addition, the received signal strength indicator is checked to serve as an indicator of network performance. The result of the study showed that wireless sensor network sensors not only improved the tracking process, as it cooperated with the process security, allowing for redundant records [22]. In some research studies, there is a lot of discussion about measuring instruments and the literature on various sensory systems for automatically detecting abnormal ozone levels [16, 35, 40]. In the following sections, we will discuss the study of the process of controlling the ozonator using sensors in the research work.

## 1. Materials and methods

To determine the normal amount of ozone in the ozonator and in the room [9], it is necessary to use a special Air Quality Monitoring Sensor Network [13, 28]. In order to live longer while maintaining health, it is necessary to monitor air quality and provide the environment with quality air [15]. Because the amount of ozone in the room is abnormal, precautions should be organized. In addition, in case of technical problems, sensors are the cause. The purpose of this scientific research work is to control the ozonator using a wireless sensor network, as well as to determine the abnormal amount of ozone. Within the framework of these issues, in-depth discussions have been carried out on the works published in many scientific publications in recent years [5]. In principle, methods based on deep learning should be developed for flexible, simple and accurate modelling of a complex technological process. Among them, for example, modeling a complex process using a series of multi-layer architectures has found a successful application. Specifically, in the following areas: traffic flow control [18], traffic speed control [16], obstacle detection for autonomous vehicles [6], health informatics [14], Water Resources Recovery [15], gesture recognition [41]. Unfortunately, the issue of air quality control is not considered.

Nwamaka U. Okafor and Declan T. Delaney's research work compared the performance of various controlled machine learning methods for calibrating low-cost IoT sensors, such as linear regression (LR) and artificial neural network (ANN). Sensors "Cairclip $O_3/NO_2$" and "cairclip $NO_2$" are positioned accordingly to determine the amount of ozone and nitrogen dioxide in an urban area. Conventional reference monitors housing the sensors provided true concentrations of gases, and these true values were used as a reference to tune the multidimensional regression models for calibrating the sensors. The sensors were calibrated using data from the first three weeks of the one-month tracking campaign. In particular, the sensor integration algorithm was used in collaboration with the Multilinear Regression (MLR) and ANN models. The performance of each calibration sample was assessed using the most recent one-week data from the field monitoring campaign using three matching metrics: mean absolute error (MAE), root mean squared error (RMSE), and detection coefficient ($R_2$). The analysis showed a significant improvement in the data quality of the cairclip $O_3/NO_2$ and cairclip $NO_2$ sensors after simple multiline regression and calibration using ANN [27].

Fouzi Harrou and his colleagues found that ozone pollution negatively affects human health and the ecosystem. In this study, he proposed an effective statistical methodology for determining abnormal ozone measurements. The research paper used the deep Belief Network model to account for nonlinear changes in ozone concentrations on Earth in conjunction with a single-class reference vector machine to determine abnormal measurements of ozone levels. The effectiveness of the methodology was evaluated using real data from the network of air quality control systems in Isere, France. The results of the research work showed the ability of the proposed strategy to detect fluctuations in ozone measurements [14]. The ontological results of the work on comparing classical and machine learning methods for spatio – temporal modeling of daily ozone concentrations are considered in the research work [2]. However, their effective solution is still a serious problem under study. The appearance of noise in sensor data has been the cause of research for a long time in sensor networks, two decades in the fields of mobile robotics and still no definitive solution is found in machine learning systems [43].

In some research papers, the most important step in the precise resolution of precision sensor networks, which is the estimation of the states of the observed variables. An analytical model has been developed to predict the relationship between resonant frequency and ozone concentration [42]. This can be done using spatio - temporal modeling. Therefore, the main goal of this study is to assess the accuracy of low-cost sensor networks. The study, testing and comparison of approaches suitable for processing space - time sensor data such as classical spatial models, spatio – temporal models and popular machine learning methods are considered [25, 38].

In the above literature on scientific research, there were no clear scientific discoveries about the process of controlling the ozonator using sensors. To this end, in the following sections, we will carry out experimental and theoretical calculations on the above research work.

## 2. The results of the experimental stand and measurement technique

The laboratory stand (Figure 1) consists of: an ozonator device based on an electric Crown discharge; a reaction chamber (RC) with a volume of 3 L; an atmospheric air com-pressor (AC) with a capacity of up to 10 l/h; a measuring transducer (MT); a signal unit (SU); gas pipeline systems and pneumatic valves.

Scope of application of the device: 1) environmental protection; 2) ensuring labor safety; 3) for scientific research purposes. Similar devices and sensors for measuring the concentration of ozone in them are currently used in medicine [3, 31].

The technological scheme of the process of controlling the ozonator using a sensor network is presented in figure 2 below. When the device is turned on in automatic mode, the level of the current value between the electrodes is checked. Recognition of the concentration of $O_3$ by the $WO_3$ gas sensor to control the amount of ozone inside the tube or room [11] if the level is lower than that of the lower sensor L1, the KL1 Valve is closed, the compressor and ozonator are turned on. When the ozone level reaches the L2 sensor, the compressor is turned off and the ozonation time is maintained. Later, when the amount of ozone decreases over time, the KL1 valve opens and the algorithm is repeated.

If, for some reason, the current sensor fails, the sensor located in the fuses and Automata is triggered. When it is activated, the algorithm is interrupted. The ozonator and compressor are turned off and the KL1 Valve is closed as well.

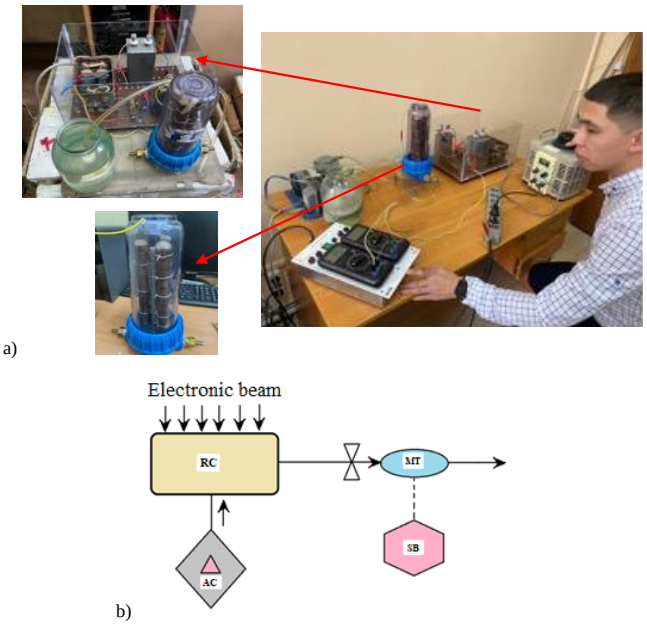


*Fig. 1. An experimental installation created based on controlling the operation of the ozonator using sensors: a) general image of the experimental installation, b) structural scheme of the experimental unit; where: RC – reaction chamber; MT – measuring transducer; SB – signal unit; AC – atmospheric air compressor. The arrows indicate the directions of gas movement*

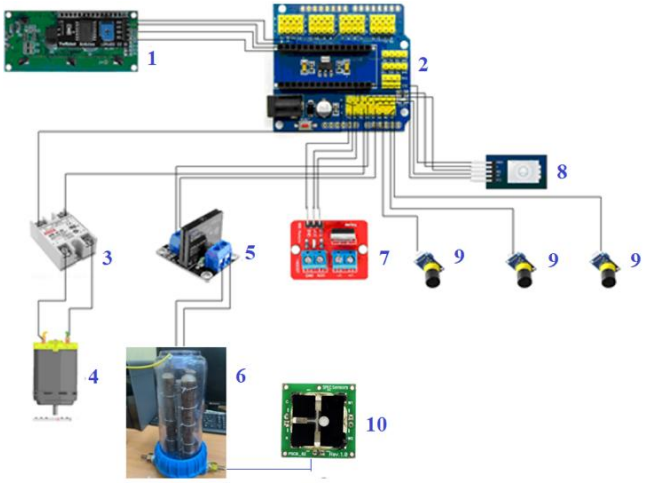


*Fig. 2. Functional scheme of the process of controlling the operation of the ozonator using sensors (1 – character LCD indicator with I2C communication module; 2 – Arduino Nano controller board 12 V; 3 – standard character indicator for amateur automation LCD 1602 with I2C Module; 4 – compressor; 5 – single-channel module of solid – state relay G3MB – 202P for switching the power of the ozonator; 6 – ozonator; 7 – MOSFET Transistor module 6WX072B; 8 – Coder KY–040 controller and Valve 12V 2A power supply for power supply; 9 – current sensors; 10 – sensor for monitoring the concentration of ozone ($O_3$)*

The "Prana Air" shown in Figure 2 (10) used ozone ($O_3$) sensors to accurately determine the ozone concentration in a certain area. Monitoring – the high concentration of ozone is harmful to human health. For the same reason, it was used to monitor the normal concentration in the room. Electrochemical sensors are the industry standard for ozone monitoring. In this type of sensor, the electric current generated by the interaction of a gas sample with an electrolyte is measured to determine the concentration of ozone in the air. The direction of the electron flow generated an electric current proportional to the concentration of the gas.

Ozone sensors "Prana Air" work on the basis of electrochemical gas detection. The sensor is used in three main components: the working electrode, the counter electrode and the ionic conductor. An ionic conductor is a bridge between two electrodes. The passage of gas through the sensor leads to the formation of a current between the electrodes, and this generated current is in the range of 0.1–3.35 μA, directly proportional to the concentration of ozone in the environment (see Figure 5). The directed flow of electrons through the wire generates an electric current directly proportional to the concentration of the gas. The gas sensor works by measuring this current between two sensors. The technical description of the sensor is given in Table 1.

*Table 1. Ozone sensor technical specifications*

| No | Parameters | Value |
|---|---|---|
| 1 | Measurement range | 0 to >20 ppm |
| 2 | Lower detection limit | < 20 ppb |
| 3 | Allowed | < 20 ppb |
| 4 | Ability to repeat | < +/- 3 % |
| 5 | Response time | Less than 15 seconds |
| 6 | Sensitivity (5 nA/ppm) | -60 +/- 10 nA/ppm |
| 7 | Working temperature range | 300 to +500C |
| 8 | Working humidity | 0–100% RH |
| 9 | Power supply | 10–50 uW |

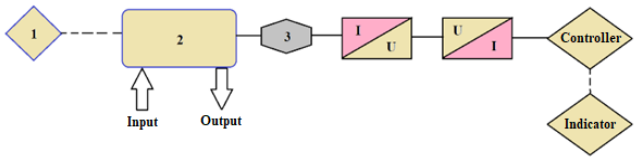


*Fig. 3. Block diagram of the ozone measuring device*

The length of the gas pipelines determines the response time of the measuring system (ozone concentration). The maximum concentration value during the experiment depends on the current strength. Repeated measurements are made only after the indicators have decreased (values from several meters to zero). The reaction chamber is a quartz flask with a height of 300 mm, an inner diameter of 140 mm and a wall thickness of 1.5 mm. The industrial ozone analyzer "OZONE-5-200 gas analyser" was used as an ozone measurement tool.

During the technological process, the ozone concentration was measured using the "OZONE – 5 – 200 gas analyser". It is an optical [7] ozone analyzer designed to determine the amount of ozone concentration in a process medium. The structural diagram of the analyzer is shown in Figure 3. The principle of operation of the gas analyzer is photometric detection (ozone at $\lambda = 2537$ A in its own absorption band). The radiation of the UV – mercury lamp (1) falls on the optical cuvette (2). Fiber integrated optical sensor based on UV LED, designed to detect ozone in the PPM and ppb ranges [8]. Through the cuvette (2), the intensity of air light that does not contain ozone is determined by the photodetector (3). A photometer based on UV LED lamps [30] when blowing an ozone-containing gas mixture through an optical cuvette (2), 253.7 nm optical absorption results in the signal generation. to obtain an exponential dependence on ozone concentration, the controller acts as a dependency. The resulting value of the ozone concentration in the gas stream is displayed in the indicator.

## 2.1. Calculation of the performance of the ozonator and its parameters

In the course of the research work, the performance of the ozonator was calculated to maintain the normal concentration of ozone in the room. According to the mass balance, the required performance of the air ozonator was calculated using the following formula:

$$G_{oz}=K\cdot C_{oz}\cdot(V/T) \quad (1)$$

where $C_{oz}$ is the concentration of ozone in the ozonating room or chamber with volume V; T is the ozonation time, $T \leq 1$ hour – this means that ozone has reacted and decomposed (AT T = 1) and AT T > 1, the ozonator produces a normal concentration. K is the coefficient reflecting the consumption of ozone for chemical interaction, thermal decomposition, etc. in practice, it is assumed that K = 5 – 10 in advance. Then, for example, to disinfect a room or chamber with a volume of 100 $m^3$ (C = 12 $mg/m^3$; $K_1$ = 5; $K_2$ = 10; T = 1 h) ozone with a yield of 6 – 12 g/h will be required. The main tasks of the ozone processing system will be as follows:

$$u_1(x,t) = A_1 + B_1 \cdot \mu\left(\frac{x}{2a_1\sqrt{t}}\right) \quad (2)$$

where $u_1(x,t)$ is the voltage distribution on the resistance surface of the ionized region. $A_1$ and $B_1$ are constants defined from the boundary conditions [1, 32]:

$$\mu(x) = \frac{2}{\sqrt{\pi}}\int_0^x e^{-\xi^2} d\xi \quad (3)$$

$$a_1 = \frac{1}{\sqrt{(R_p+R_e)\,C_b}} \quad (4)$$

$x = \xi$ at the ionization boundary condition:

$$U_{power\ supply} + B_1 \cdot \mu\left(\frac{\xi}{2a_1\sqrt{t}}\right) = u_1(\xi,t) \quad (5)$$

the formula (5) is valid when the microregration boundary moves (ionization) according to a known pattern:

$$\xi = \psi\sqrt{t}\,, m \quad (6)$$

where $\psi$ is some stability, $m/s^{1/2}$; $t$ is the moment of the start time of the surface microrastructure, s.

Let's introduce markup:

$$\psi/2a_1 = \beta \quad (7)$$

The voltage distribution on the resistance surface in the microrastructure region is determined by the formula:

$$u_1(x,t) = U_{power\ supply} - \frac{U_{power\ supply}}{\mu(\beta)} \cdot \mu\left(\frac{x}{2a_1\sqrt{t}}\right), x \leq \xi \quad (8)$$

to differentiate the formula with respect to $x$, we obtain the following equation, which is the electric field strength in the microregration region:

$$E_1(x,t) = -\frac{U_{power\ supply}}{\sqrt{\pi}a_1\sqrt{t}\mu(\beta)} exp\left[-\left(\frac{x}{2a_1\sqrt{t}}\right)^2\right] \quad (9)$$

The value of the electric field strength at the ionization boundary $x = \xi$ and $t = t_\mu$ was determined as follows:

$$\left|E_1(\xi,t_\mu)\right| = \frac{U_{power\ supply}}{\sqrt{\pi}a_1\sqrt{t_\mu}\,\mu(\beta)} exp(-\beta^2) = E_0\,, W/m \quad (10)$$

where $t_\mu$ is the time of formation of the microrastructure, s. $E_0 = 2.45\cdot10^6$ V/m is the threshold intensity of the onset of air ionization.

[1, 32] in his scientific works, he calculated $\beta(t_\mu)=1/\sqrt{2}$. Taking into account these formulas (10), (6), we get the expression for determining time. That is, the formation of a micro-discharge depending on the voltage of the power supply:

$$t_\mu = \frac{U^2_{power\ supply}}{E_0^2}\cdot\frac{exp(-2\beta^2)}{\pi\mu^2(\beta)}\left(R_\text{p}+R_e\right)C_b = 0.25\left(\frac{U_{power\ supply}}{E_\text{p}}\right)^2\left(R_\text{p}+R_e\right)C_b \quad (11)$$

Taking into account the expressions (9) and (10), we subtract (11) from the equation. That is, the formula for determining the position of the ionization boundary:

$$\xi = \frac{U_{power\ supply}}{E_0}\cdot\frac{exp(-\beta^2)}{\sqrt{\pi}\mu(\beta)}\cdot 2\beta = \frac{U_{power\ supply}}{\sqrt{2}E_0} \quad (12)$$

From the formula (12), it can be seen that in the first approximation is a geometric solution. The microrastructure is independent of the resistance of the electrodes and the formation time, as described by the formula (11), which accounts for the resistance of the high electrodes ($R_e$).

Let us give a qualitative assessment of the microrastric current depending on the values of the resistance of the high electrode and the length of the microrastric. Because the data on such microrastructure currents have not been studied in the works mentioned above [1, 32].

Given the symmetry of the development of microrastructures in all directions of the needle electrode, the total current of the surface microrastructure near the electrode region can be determined by the approximate formula:

$$I(0,t) = 2\text{i}(0,t)b_p = -2\frac{E_1(0,t)}{R_\text{p}+R_e}b_p \quad (13)$$

where $b_\text{p}$ is the width of the discharge area, m.

Electric field strength at the electrode boundary, V/m:

$$E_1(0,t) = -\frac{U\ power\ supply}{\sqrt{\pi}a_1\sqrt{t}\mu(\beta)} \quad (14)$$

In formula (13), the coefficient "2" is due to the first approximation, which can be considered as a real axially symmetric microrasry (shown in figure 1a) and its width can be assumed to be equal to $b_p = 2\xi = 2\psi\sqrt{t}$ for the microrasry needle electrode. The maximum value of the current at the length of the microrastructure is reached by $x = \xi$ ($\beta = 1/\sqrt{2}$), which can be determined by the formula:

$$I_m = 3.3U_{power\ supply}a_1C_b\beta\cdot 2a_1 \approx 4.7\frac{U_{power\ supply}}{R_\text{p}+R_e} \quad (15)$$

according to the expression, the current remains unchanged in the process of microrasry formation. In real conditions, the current in the microrasterate increases from zero to the maximum value. This is explained by the presence of a microrism in a circuit with inductive and surface resistance. The limit value of the specific surface resistance in it is $\rho_S = 10^9$ Ohms. It increases to the value of the surface resistivity in the discharge area $\rho_S = 10^4$ Ohms. To demonstrate the positive effect of using a high electrode resistance, the resistance of the electrodes should be in accordance with $R_\text{e}$ and the resistance of the microrastructure surface should be $R_\text{p} \approx 10^4$ Ohms.

For further theoretical calculations, we will take the following: $R_\text{e} \approx R_\text{p} = 10^4$ Ohms. Then we obtain the following results for high-resistance electrodes with a voltage of 5–10 kV:

– microdischarge length

$$\xi = \frac{U_{power\ supply}}{\sqrt{2}E_0} = \frac{10^4}{\sqrt{2}\cdot 2.45\cdot 10^6} = 2.9\cdot 10^{-3} \quad (16)$$

– parameter value

$$\psi = 2a_1\beta = \frac{2\beta}{\sqrt{(R_\text{p}+R_e)C_b}} \quad (17)$$

where the specific capacitance of the dielectric resistance, μ/m$^2$ can be calculated as follows:

$$C_b = \frac{\varepsilon\varepsilon_0}{d}$$

$d$ – the thickness of the dielectric barrier, m.

Let's take the values of the parameters of the dielectric barrier of the ozonator $\varepsilon = 3.5$, $d = 10^{-3}$ m, where $C_\text{b} \approx 3\cdot 10^{-8}$ μ/m$^2$, $\psi \approx 50$ (Figure 4);

The microrastructure formation time is determined using the:

$$t_\mu = (\xi/\psi)^2 \approx 3.3\cdot 10^{-9} \quad (18)$$

$$r_{mic} + r_B = \frac{U_{power\ supply}}{I_m} = \frac{1}{4.7}\left(R_\text{p}+R_e\right) \quad (19)$$

there $r_{mic} = R_\text{p}/4.7 = 2100$ Ohms – efficiency of microdischarge interference.

To use the sensor, it is necessary to directly measure the temperature of the metal surface during the catalytic dissociation of ozone [39]. Similarly, it is worth considering the physical-based characteristic of noise reactions in metal-oxide gas sensors [4].

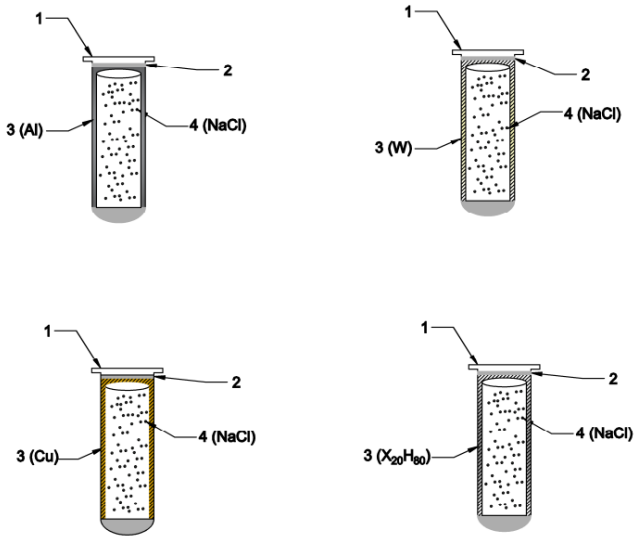


*Fig. 4. Structural diagram of a laboratory ozonator, where: 1 – the dielectric material between the electrodes is made of tempered glass; 2 – fluoroplast; 3 – electrodes made of different material (Al, W, Cu,X20H80); 4 – table salt (NaCl)*

Since the microrasry has axial symmetry, to be more accurate, calculating as $b_\text{p}$ the width through which the microrasry current passes, it is necessary to take the circumference of the electronic Avalanche (streamer). This is the beginning of the microrasration process:

$$\xi_0 = 2\pi r_0 \quad (20)$$

where $r_0 \approx 0.5\cdot 10^{-3}$ m is the radius of the electronic avalanche or streamer [33].

From the formula (13), taking into account the maximum value of the microrastructure current, we can obtain the expression:

$$I_m = 1.65\frac{E_0 2\pi r_0}{R_\text{p}+R_e} \approx 10.4\frac{E_0 r_0}{R_\text{p}+R_e} \quad (21)$$

If $R_\text{e} = 0$, $R_\text{p} = 10^4$ Ohms then $I_\text{m} = 1.27$ μA and if $R_\text{e} = R_\text{p} = 10^4$ Ohms then $I_\text{m} = 0.64$ μA, which is close to the known experimental data, where $0.1\ \mu\text{A} < I_\text{m} < 1\ \mu\text{A}$.

The minimum voltage that occurs in a microdischarge:

$$U_{min} = I_m r_{mic} = 0.64\cdot 2100 \approx 1.35\ kV \quad (22)$$

The working voltage of the sinusoidal power supply is equal to:

$$U_{power\ supply} = 1.35/\sqrt{2} = 0.96\ kV \quad (23)$$

Let's calculate the diameter of the area of the microrastructure near the axial barrier (symmetry).

$t = t_\mu$ for:

$$d_b(t_\mu) = 2(r_e+\xi) = 2\left(r_e + \frac{U_{power\ supply}}{\sqrt{2}E_0}\right) \quad (24)$$

where $r_\text{e}$ is the radius of the electrode. At this point $U_{\text{power source}} = 5$–$10$ kV, $r_\text{e} = 0.5$ mm, $d_\text{b}(t_\mu) = 6.8$ mm.

## 2.2. Experimental research results

The following experimental results were obtained on the process of controlling the ozonator using a sensor network. At first, the change in ozone concentration depending on the current strength was considered (Figure 5).

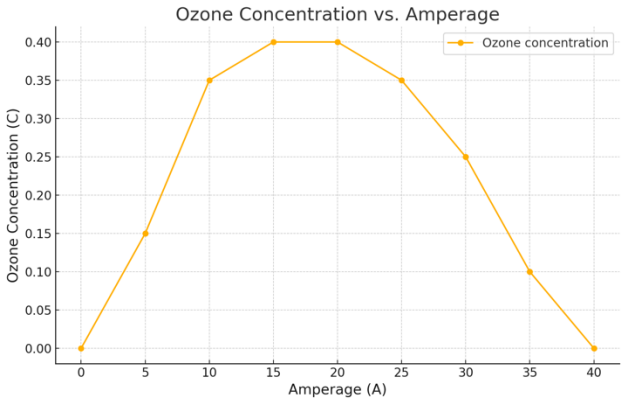


*Fig. 5. The relationship between amperage and ozone concentration*

As can be seen from Figure 5, it can be seen that the concentration of ozone up to 0.1–0.75 μA is normal, and the concentration of ozone up to 0.75–4.75 μA is sharply increased, and the concentration of ozone up to 4.75–20 μA is normal. During the experimental research work, it was observed that the ozone concentration immediately decreased due to the formation of an arc discharge between the electrodes when the current increased by 20 μA. This is because the ozone concentration immediately dropped due to the increase in temperature inside the chamber. The volt-ampere characteristic of the ozonator is shown in Figure 6.

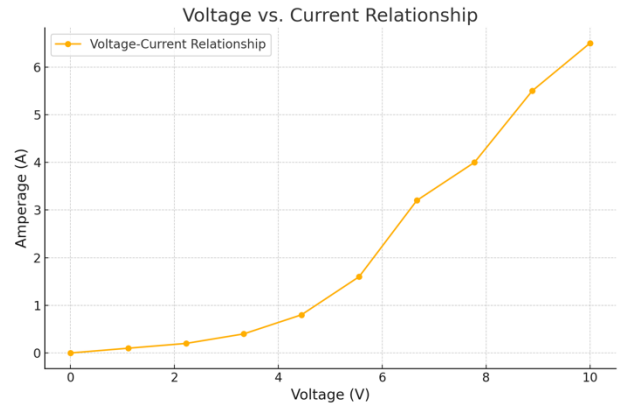


*Fig. 6. Ozonator volt-ampere description*

What we observe from the volt – ampere characteristic of the ozonator in Figure 6 can be traced the linear relationship between current and voltage. However, during the experiment, it was observed that the voltage did not change from 1886.37 to 2642.58 kV (because the resistance between the electrodes is very large "several MMS"), and at 2642.58–4155 kV we observed "quiet discharge", at 4155–5664.65 kV "Crown discharge", at 5664.65–7174.854 kV "arc discharge". Sensors were used to maintain the voltage values in the range of 4155–5664.65 kV "Crown discharge" Figure 2 above.

## 2.3. Mathematical model of research results

The electrical diagram of the ozonator is shown in Figure 7, and its algorithm and program code are shown in Figure 8. By means of the voltage coming from the source of the node, it is possible to change the magnitude of the current passing on the corona electrodes in the ozonator.

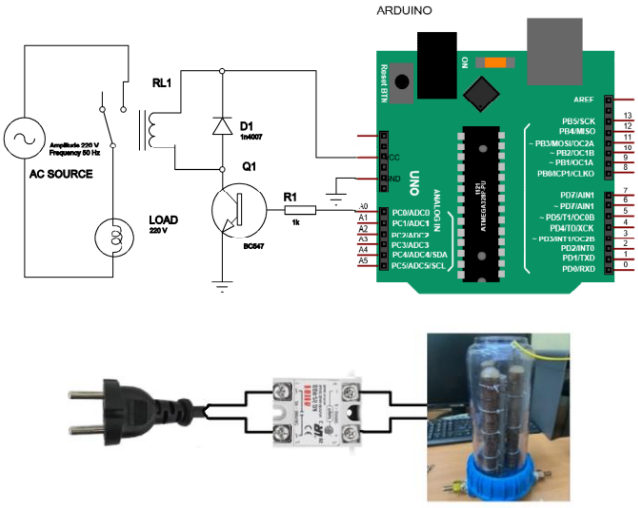


*Fig. 7. Electrical circuit of the ozonator (rolled up on the ARDUINO platform)*

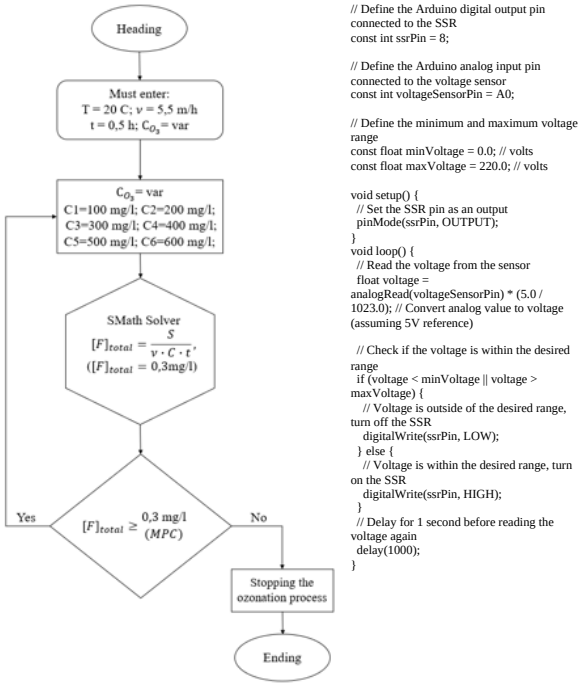


*Fig. 8. Algorithm of the process of controlling the ozonator using a sensor network*

## 3. Discussion of research work

To control the operation of the ozonator using electronic sensors, the relationship between the rate of ozone formation inside the chamber and the air temperature formed by the current along the corona discharge [33] in it can be nonlinear. The data collected in the control unit is used to improve the quality of ozone and other products and to maintain the quality of sensor data calibration over the life of the sensor [34]. To analyse the process, let's first consider the general equation of its photochemical formation [20, 29].

$$\mathrm{CO} + \mathrm{CH_4} + RH + NO \xrightarrow{h\nu, H_2O, O_2} fH_2CO + KO_3 + NO_2 + \mathrm{P} \quad (25)$$

where, $f$ – stoichiometric coefficient of hydrocarbon conversion; $K$ – coefficient of ozone synthesis at the ozonator outlet it depends on the concentration of nitrogen oxides; P – products of photochemical reactions, which are aerosol particles formed during the interaction of gas components.

The physical meaning of the general equation is as follows: primary impurities CO – carbon monoxide, $CH_4$ – methane, RH – non-methane hydrocarbons, no-nitrogen oxide, water vapor ($H_2O$) and oxygen ($O_2$) enter the atmosphere and are converted under

the influence of ultraviolet light (*hv*). Similarly, $H_2CO$-formaldehyde, $O_3$ – ozone, $NO_2$ – nitrogen dioxide and P – reaction products (typical aerosols). Table 2 below lists the reactions and some constants in the ozone processing system in the ozonator chamber [21].

*Table 2. Constants with some photochemical reactions in the Ozone Treatment System [2]*

| Reaction | Stability |
|---|---|
| $O + O_2 + M \rightarrow O_3 + M$ | $6.0{\cdot}10^{-34}(T/300)^{-2.6}$ |
| $H + O_2 + M \rightarrow HO_2 + M$ | $5.4{\cdot}10^{-32}(T/300)^{-1.8}$ |
| $O + HO_2 \rightarrow HO + O_2$ | $2.7{\cdot}10^{-11}\exp(224/T)$ |
| $O + H_2O_2 \rightarrow HO + HO_2$ | $1.4{\cdot}10^{-12}\exp(-2000/T)$ |
| $HO + HO + M \rightarrow H_2O_2 + M$ | $6.9{\cdot}10^{-31}(T/300)^{-0.8}$ |
| $O + NO + M \rightarrow NO_2 + M$ | $1.0{\cdot}10^{-31}(T/300)^{-1.6}$ |
| $O + NO_2 \rightarrow O_2 + NO$ | $5.5{\cdot}10^{-12}\exp(188/T)$ |
| $HO + CH_4 \rightarrow H_2O + CH_3$ | $1.85{\cdot}10^{-12}\exp(-1690/T)$ |
| $HO + C_2H_4 + M \rightarrow C_2H_4OH + M$ | $8.6{\cdot}10^{-29}(T/300)^{-3.4}$ |
| $HO + C_2H_6 \rightarrow H_2O + C_2H_5$ | $6.9{\cdot}10^{-12}\exp(-1000/T)$ |
| $HO + C_3H_6 + M \rightarrow C_3H_6OH + M$ | $8.0{\cdot}10^{-27}(T/300)^{-3.5}$ |
| $HO + C_3H_8 \rightarrow H_2O + C_3H_7$ | $7.6{\cdot}10^{-12}\exp(-585/T)$ |
| HO + α-pinene → products | $1.2{\cdot}10^{-11}\exp(440/T)$ |
| $HO + CO \rightarrow H + CO_2$ | $9.1{\cdot}10^{-19}{\cdot}T^{1.77}\exp(580/T)$ |
| $NO_3 + C_2H_4 \rightarrow$ products | $3.3{\cdot}10^{-12}\exp(-2880/T)$ |
| $NO_3 + C_3H_6 \rightarrow$ products | $4.6{\cdot}10^{-13}\exp(-1155/T)$ |
| $NO_3 + n\text{-}C_4H_{10} \rightarrow$ products | $2.8{\cdot}10^{-12}\exp(-3280/T)$ |
| $NO_3$ + α-pinene → products | $1.2{\cdot}10^{-12}\exp(490/T)$ |

The constants of some photochemical reactions presented in Table 2 were observed in the course of experimental research work (see Figure 9).

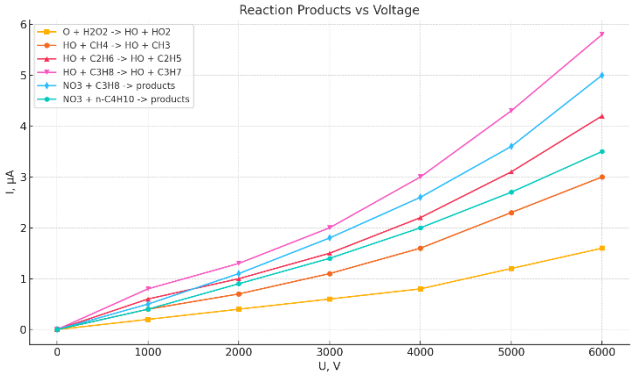


*Fig. 9. Reactions caused by photochemical radiation due to voltage and current inside the ozonator chamber*

Thus, the amount of ozone generated depends on the composition and concentration of other gases and light radiation. In addition, during photochemical generation, the process can branch out and various compounds are involved in the reaction. In this case, the constants of the reactions also changed, because most of them depend on the temperature in the chamber caused by the current (Figure 10).

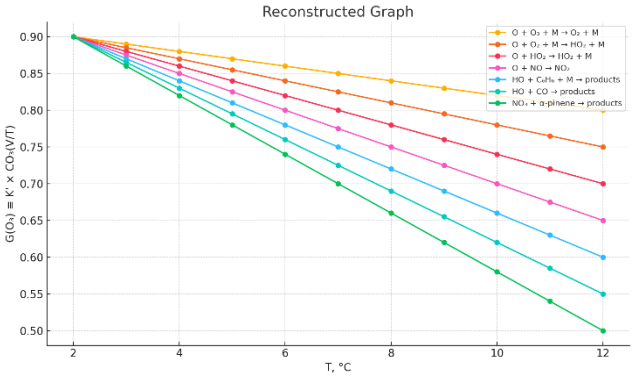


*Fig. 10. Changes in ozone and some reactions during the process due to temperature caused by discharge inside the ozonator chamber*

How the constant of the reaction rate changes when the temperature generated by the action of the current inside the ozonator changes can be observed in Figure 10. The studies carried out have shown that with an increase in temperature, the reaction rate can both increase and decrease. Therefore, all selected reactions were divided into two groups: those in which the reaction rate decreases and those that increase due to the increase in temperature.

From Figure 10, it can be seen that due to the increase in temperature, reactions slow down and the reaction rate can vary up to 3 times in the range of 2–12°C. And accordingly, for some part of some reactions, their speed increases up to 10 times in the same range. This indicates that the amount of ozone formed due to the composition of progenitor gases is nonlinear due to the increase in air temperature.

Thus, during the experiment, it was observed that if the oxygen or air temperature in the ozonator exceeds 6–12°C, the ozone concentration immediately drops below. Therefore, during the research work, special current sensors were applied to the camera (Figure 2: 9-current sensors).

According to previously reviewed sources, when controlling the operation of the ozonator using electronic sensors, no specific data on temperature changes in the chamber using current sensors were detected. The peculiarity of the research work is that during the discharge of the corona of electric discharge in the chamber, that is, the lower the temperature, the higher the concentration of ozone. For example, the temperature in a chamber at 12°C has a velocity of 1.6 μg/(g·h), and at 6°C it is 18.8 μg/(g·h). It was found that a change in temperature of 6°C leads to an increase in the concentration of this ozone by 11.75 times.

Temperature fluctuations in the camera have a predictable, easily compensated effect on the sensor signal (Figure 10). The figure shows the dependence of the research result on temperature. This information was collected at a constant humidity of 40–50% RH. This very uniform and repetitive effect is easily compensated for in hardware or software. The result of the study is presented in Figure 11 below.

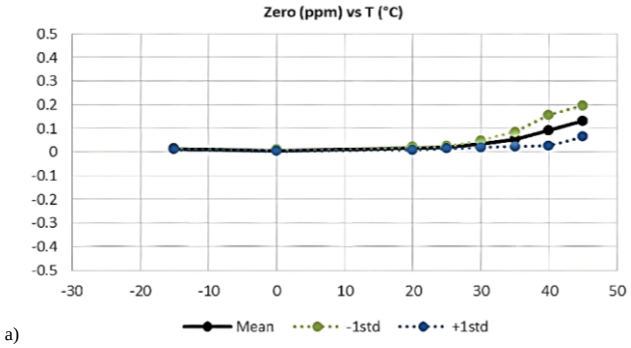


a)

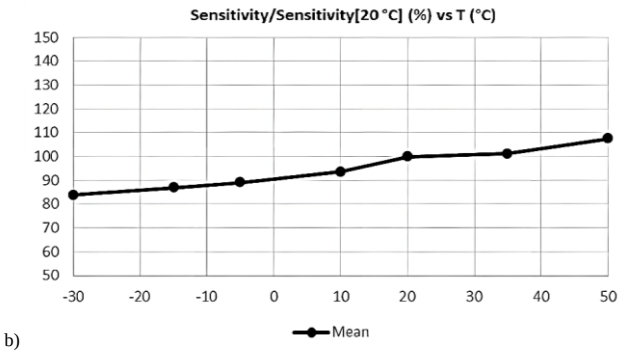


b)

*Fig. 11 (part 1). Results of the experiment: a) influence of temperature, b) influence of temperature on sensitivity, c) changes in ozone ($O_3$) depending on time*

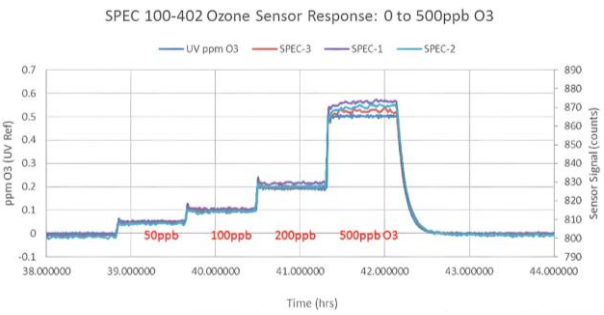


c)

*Fig. 11 (part 2). Results of the experiment: a) influence of temperature, b) influence of temperature on sensitivity, c) changes in ozone ($O_3$) depending on time*

During the study, it was found that controlling the operation of the ozonator using sensors gives a safe and effective solution during the process.

## 4. Conclusion

Summarizing the scientific research work, temperature fluctuations in the ozonator chamber have a predictable and easily compensated effect on the sensor signal. The operation of the ozonator and the gas that does not meet the maximum permissible concentration of ozone in the room around it is immediately monitored by a sensor that allows you to adjust it to normal mode. Information is easily compensated in software. The layout of the device is laid out on the ARDUINO platform and software codes are written.

During the study of the process of measuring and controlling the operation of the ozonator using electronic sensors, the current strength, temperature and other physical and chemical parameters passing through the corona electrodes were calculated and discussed theoretically and experimentally. In it, according to measurement data in the background area, the dependence of the rate of ozone formation in the ozonator on air temperature was studied. It turned out that it is not linear. So, it was found that the concentration of ozone around the electrode in the ozonator is directly proportional to the decrease in temperature (for example, at 1°C – corresponds to an increase in the concentration of 5 $\mu g/m^3$). During the research work, theoretical calculations were carried out on the data obtained in the experiment. In particular, sensors were used during the technological process in order to monitor and study the concentration of ozone in the room and in the ozonator.

## References


[1] Abdykadyrov A. et al.: Purification of surface water by using the corona discharge method. Mining of Mineral Deposits, 18 (1), 2024, 125–137. [https://doi.org/10.33271/mining18.01.125].

[2] Abdykadyrov A., Kalandarov P., Marxuly S., Zhunussov K., Sharipova G., Sabyrova A., Akylzhan P., Uzak M.: Study of the process of neutralization of microorganisms in drinking water exposed to environmental problems. Water Conservation and Management, 8(3), 2024, 352–361 [https://doi.org/10.26480/wcm.03.2024.352.361].

[3] Agarwala R., Wang P., Bishop H. L., Dissanayake A., Calhoun B. H.: A 0.6V 785-nW Multimodal Sensor Interface IC for Ozone Pollutant Sensing and Correlated Cardiovascular Disease Monitoring. IEEE Journal of Solid-State Circuits 56(4), 2021, 1058–1070 [https://doi.org/10.1109/JSSC.2021.3057229].

[4] Contaret T., Seguin J.-L., Menini P., Aguir K.: Physical-Based Characterization of Noise Responses in Metal-Oxide Gas Sensors. IEEE Sensors Journal 13(3), 2013, 980–986 [https://doi.org/10.1109/JSEN.2012.2227707].

[5] Costilla-Reyes O., Scully P., Ozanyan K. B.: Deep neural networks for learning spatio-temporal features from tomography sensors. IEEE Transactions on Industrial Electronics 65(1), 2018, 645–653 [https://doi.org/10.1109/TIE.2017.2716907].

[6] Dairi A., Harrou F., Senouci M., Sun Y.: Unsupervised obstacle detection in driving environments using deep-learning-based stereovision. Robotics and Autonomous Systems 100, 2018, 287–301.

[7] Degner M., Damaschke N., Ewald H., Lewis E.: High resolution LED-spectroscopy for sensor application in harsh environment. IEEE Instrumentation & Measurement Technology Conference Proceedings. USA, Austin, TX, 2010, 1382–1386 [https://doi.org/10.1109/IMTC.2010.5488239].

[8] Degner M., Damaschke N., Ewald H., O'Keeffe S., Lewis E.: UV LED-based fiber coupled optical sensor for detection of ozone in the ppm and ppb range. IEEE SENSORS, Christchurch, New Zealand, 2009, 95–99 [https://doi.org/10.1109/ICSENS.2009.5398230].

[9] Doll T., Fuchs A., Eisele I., Faglia G., Groppelli S., Sberveglieri G.: Room temperature ozone sensing with conductivity and work function sensors based on indium oxide. Proceedings of International Solid State Sensors and Actuators Conference (Transducers '97), 1997 [https://doi.org/10.1109/SENSOR.1997.613716].

[10] Egorov I., Esipov V., Remnev G., Kaikanov M., Lukonin E., Poloskov A.: A high-repetition rate pulsed electron accelerator. IEEE Transactions on Dielectrics and Electrical Insulation 20(4), 2013, 1334–1339 [https://doi.org/10.1109/TDEI.2013.6571453].

[11] Faleh R., Othman M., Kachouri A., Aguir K.: Recognition of O3 concentration using WO3 gas sensor and principal component analysis. 1st International Conference on Advanced Technologies for Signal and Image Processing (ATSIP), Sousse, Tunisia, 2014, 322–327 [https://doi.org/10.1109/ATSIP.2014.6834629].

[12] Fechete A. C., Wlodarski W. B., Kalantar-zadeh K., Holland A. S., Wisistsora-at A.: Ozone Sensors based on Layered SAW Devices with: InOx/SiNx/36° YX LiTaO3 Structure. TENCON 2005–2005 IEEE Region 10 Conference, Melbourne, 2005, 1–4 [https://doi.org/10.1109/TENCON.2005.301325].

[13] Ghazaly C., Guillemot M., Castel B., Langlois E., Etienne M., Hebrant M.: Real-Time Optical Ozone Sensor for Occupational Exposure Assessment. 20th International Conference on Solid-State Sensors, Actuators and Microsystems & Eurosensors XXXIII (TRANSDUCERS & EUROSENSORS XXXIII), Berlin, Germany, 2019, 1403–1406 [https://doi.org/10.1109/TRANSDUCERS.2019.8808516].

[14] Harrou F., Dairi A., Sun Y., Senouci M.: Reliable detection of abnormal ozone measurements using an air quality sensors network. IEEE International Conference on Environmental Engineering (EE), Milan, Italy, 2018 [https://doi.org/10.1109/EE1.2018.8385265].

[15] Harrou F., Nounou M., Nounou H.: Statistical detection of abnormal ozone levels using principal component analysis. International Journal of Engineering & Technology 12(6), 2012, 54–59.

[16] Jia Y., Wu J., Du Y.: Traffic speed prediction using deep learning method. IEEE 19th International Conference Intelligent Transportation Systems (ITSC), 2016, 1217–1222.

[17] Kanokwan R., Chaiwas S., Nantivatana P., Kocharoen P., Thaenkaew S., Tansriwong S.: Efficiency evaluation of ozone gas concentration generation by commercial ozone generator for disinfection in residential buildings. International Electrical Engineering Congress (iEECON), Khon Kaen, Thailand, 2022 [https://doi.org/10.1109/iEECON53204.2022.9741631].

[18] Koesdwiady A., Soua R., Karray F.: Improving traffic flow prediction with weather information in connected cars: A deep learning approach. IEEE Transactions on Vehicular Technology 65(12), 2016, 9508–9517.

[19] Latif T., Dieffenderfer J., Tanneeru A., Lee B., Misra V., Bozkurt A.: Evaluation of Environmental Enclosures for Effective Ambient Ozone Sensing in Wrist-worn Health and Exposure Trackers. IEEE Sensors. Australia, Sydney, 2021 [https://doi.org/10.1109/SENSORS47087.2021.9639530].

[20] Lunin V. V., Popovich M. P., Tkachenko S. N.: Physical chemistry of ozone. Max Press, Moscow, 2019.

[21] Lunin V. V., Samoilovich V. G., Tkachenko S. N., Tkachenko I. S.: Theory and practice of obtaining and applying ozone. Moscow University Press, Moscow 2016.

[22] Luqueta G. R., Santos E. D., Pessoa R. S., Maciel H. S.: Wireless Sensor Network to Monitoring an Ozone Sterilizer. IEEE Latin America Transactions 14(5), 2016, 2167–2174 [https://doi.org/10.1109/TLA.2016.7530410].

[23] Maximum permissible concentrations (MPC) of pollutants in the atmospheric air of populated areas. Hygienic standards 2.1.6.1338-03. Ministry of Health of Russia, Moscow 2003 [https://files.stroyinf.ru/Data2/1/4294814/4294814669.pdf].

[24] Mischo M., Bitterling M., Himmerlich M., Krischok S., Ambacher O., Cimalla V.: Seebeck ozone sensors. The 17th International Conference on Solid-State Sensors, Actuators and Microsystems (Transducers & Eurosensors XXVII), 2013 [https://doi.org/10.1109/Transducers.2013.6627100].

[25] Mukhopadhyay S., Sahu S. K.: A Bayesian spatiotemporal model to estimate long-term exposure to outdoor air pollution at coarser administrative geographies in England and Wales. Journal of the Royal Statistical Society Series A: Statistics in Society 181(2), 2018, 465–486 [https://doi.org/10.1111/rssa.12299].

[26] Nawahda A.: An assessment of adding value of traffic information and other attributes as part of its classifiers in a data mining tool set for predicting surface ozone levels. Process Safety and Environmental Protection 99, 2016, 149–158.

[27] Okafor N. U., Delaney D. T.: Application of Machine Learning Techniques for the Calibration of Low-cost IoT Sensors in Environmental Monitoring Networks. IEEE 6th World Forum on Internet of Things (WF-IoT). USA, New Orleans, LA, 2020 [https://doi.org/10.1109/WF-IoT48130.2020.9221246].

[28] O'Keeffe S., Fitzpatrick C., Lewis E.: Ozone Measurement Using Optical Fibre Sensors in the Visible Region. IEEE SENSORS, Irvine, CA, USA, 2005, [https://doi.org/10.1109/ICSENS.2005.1597810].

[29] Pan C., Yan B., Flynn L., Beck T., Jin X., Buckner S.: Ozone Mapper Profiler Suite Nadir Profiler Degradation. IEEE International Geoscience and Remote Sensing Symposium (IGARSS 2022). Malaysia, Kuala Lumpur, 2022, 7348–7350 [https://doi.org/10.1109/IGARSS46834.2022.9883681].

[30] Parameswaran K. R., Sonnenfroh D. M.: Compact ozone photometer based on UV LEDs. 23rd Annual Meeting of the IEEE Photonics Society, Denver, CO, USA, 2010, 375–376 [https://doi.org/10.1109/PHOTONICS.2010.5698916].

[31] Petani L., Wickersheim D., Koker L., Reischl M., Gengenbach U., Pylatiuk C.: Experimental Setup for Evaluation of Medical Ozone Gas Sensors. IEEE Sensors Applications Symposium (SAS), Sundsvall, Sweden, 2022 [https://doi.org/10.1109/SAS54819.2022.9881340].

[32] Pichugin Yu. P.: Evaluation of geometric and temperature parameters of micro-discharges in a barrier discharge. Bulletin of the Chuvash University 3, 2011, 102–107.

[33] Rahmat S. et al.: The Correlation Among Ozone Gases, Hissing Frequency, and Ultraviolet Light in Corona Effects. 2nd International Conference on Electronic and Electrical Engineering and Intelligent System (ICE3IS). Indonesia, Yogyakarta, 2022, 74–78 [https://doi.org/10.1109/ICE3IS56585.2022.10010024].
[34] Raiser Yu. P.: Physics of a gas discharge. Scientific publication. Publishing House "Intellect", Dolgoprudny 2009.
[35] Ravì D., Wong C., Deligianni F., Berthelot M., Andreu-Perez J., Lo B., Yang G.-Z.: Deep learning for health informatics. IEEE Journal of Biomedical and Health Informatics 21(1), 2017, 4–21.
[36] Rissanen M. P. et al.: The formation of highly oxidized multifunctional products in the ozonolysis of cyclohexene. Journal of the American Chemical Society 136(44), 2014, 15596–15606.
[37] Shaban K. B., Kadri A., Rezk E.: Urban air pollution monitoring system with forecasting models. IEEE Sensors Journal 16(8), 2016, 2598–2606.
[38] Shaddick G., Wakefield J.: Modelling daily multivariate pollutant data at multiple sites. Journal of the Royal Statistical Society: Series C (Applied Statistics) 51(3), 2002, 351–372.
[39] Sung T.-L.: Direct Measurement of Metal Surface Temperature During Catalytic Dissociation of Ozone for Sensor Application. IEEE Transactions on Plasma Science 42(12), 2014, 3842–3846 [https://doi.org/10.1109/TPS.2014.2350000].
[40] Suryono S., Khuriati A.: Mobile Measurement System of Ozone Concentration in Urban Areas. Third International Conference on Informatics and Computing (ICIC), Palembang, Indonesia, 2018 [https://doi.org/10.1109/IAC.2018.8780449].
[41] Wang J., Zhang X., Gao Q., Yue H., Wang H.: Device-free wireless localization and activity recognition: A deep learning approach. IEEE Transactions on Vehicular Technology 66(7), 2017, 6258–6267.
[42] Wang Z. et al.: Ozone senosr using ZnO based film bulk acoustic resonator. 16th International Solid-State Sensors, Actuators and Microsystems Conference, China, Beijing, 2011, 1124–1127 [https://doi.org/10.1109/TRANSDUCERS.2011.5969275].
[43] Wen H., Xiao Z., Markham A., Trigoni N.: Accuracy estimation for sensor systems. IEEE Transactions on Mobile Computing 14(7), 2015, 1330–1343.

**M.Sc. Sunggat Marxuly**
e-mail: sungat50@gmail.com

Master of Technical Sciences, doctoral student. Senior lecturer at Kazakh National Research Technical University named after K. Satbayev. Winner of the award "Best University Teacher 2023".
He has more than 90 scientific articles, 4 patents for inventions, 6 teaching aids, 7 methodological manuals.

https://orcid.org/0000-0002-7330-5927

**C.Sc. Katipa Chezhimbayeva**
e-mail: k.chezhimbayeva@satbayev.university

Candidate of Technical Sciences. Associate professor at the Almaty University of Power Engineering and Telecommunications named after G.Daukeev.

https://orcid.org/ 0000-0002-1661-2226

**C.Sc. Askar Abdykadyrov**
e-mail: a.abdykadyrov@satbayev.university

Candidate of Technical Sciences. Associate professor at the Kazakh National Research Technical University named after K. Satbayev. Winner of the award "Best University Teacher 2023".
He has more than 90 scientific articles, 4 patents, 4 teaching aids.

https://orcid.org/0000-0003-1143-4675

**Ph.D. Nurzhigit Smailov**
e-mail: n.smailov@satbayev.university

Ph.D., professor at the Kazakh National Research Technical University named after K. Satbayev. Winner of the award "Best University Teacher 2022".
He has more than 50 scientific articles, 4 patents, 2 teaching aids.

https://orcid.org/0000-0002-7264-2390